Supplementary Information

Engineered partially open-cage fluorinated polyhedral oligomeric silsesquioxane hybrid nanoparticle aggregates for surfaces with super-repellency to widespread liquids

Boxu Chen,‡[ac] Xilin Lin,‡[ab] Mingjin Yang,[ab] Zonglin You,[c] Wenfeng Liu,*[c] Hailin Meng,[ab] Yahong Zhou,[d] Hai Yuan[ab] and Jingwen Liao*[ab]*

[a.] Frontier Science and Technology Research Center, Bioengineering Research Center, Guangzhou Institute of Advanced Technology, Guangzhou 511458, China. E-mail: mj.yang@giat.ac.cn; jw.liao@giat.ac.cn

[b.] Shenzhen Institutes of Advanced Technology, Chinese Academy of Sciences, Shenzhen 518055, China

[c.] School of Biotechnology and Health Sciences, Wuyi University, Jiangmen 529020, China. E-mail: wyuchemlwf@126.com

[d.] CAS Key Laboratory of Bio-inspired Materials and Interfacial Science, Technical Institute of Physics and Chemistry, Chinese Academy of Sciences, Beijing 100190, China

‡ These authors contributed equally to this work and should be considered co-first authors.

Experimental (partly)

Chemicals

If not otherwise specified, the chemicals of analytical grade were purchased from Aladdin Chem Co., and used without further treatment. The waterborne polyacrylate resins, solventborne polyurethane resins, fluoropolymer resins (waterborne and solventborne) were supplied by Wuxi Honghui New Materials Technology Co., Degussa Co. and DuPont Co., respectively.

Characterization and tests

Characterization: NMR spectroscopy (Magritek GmbH Spinsolve 60, Germany) was utilized to qualitatively characterize poc-FPOSS-2OH (^{1}H-NMR: 500 MHz, C_6D_6/C_6F_6; ^{29}Si-NMR: 400 MHz, C_2D_6O). Both the XPS (Kratos Axis Ultra DLD, Britain), CHN analyzer (PerkinElmer 2400 Series II, USA) and Fourier-transform infrared (FTIR) spectroscopy (Bruker Vector 33, Germany) were applied to analyze the chemical composition of as-obtained products. XRD spectroscopy (BrukerD8 Advanced, Germany) was used to record the crystalline states of specimens. Both FE-SEM (ZEISS Ultra 55, Germany) and HR-TEM (JEOL JEM-2100F, Japan) were employed to probe the topography of specimens. Liquid chromatography (Thermo Scientific UltiMate™ 3000 UHPLC, USA)-tandem high resolution mass spectrometry (ThermoFisher Scientific Q Exactive, Germany) was employed to determine the molecular weight of poc-FPOSS-2OH. Thermogravimetric analyzer (Netzsch TG 209, F3, Germany) was used to record the weight loss behavior of specimens (30~800℃ with 10 °C min^{-1}, N_2 atmosphere at a rate of 20 mL min^{-1}).

Contact angle measurement: The contact/roll-off angle measurements of specimens were performed using a surface contact angle analyzer (KSV Helsinki CAM200, Finland) with a 2 μL of liquid droplet at ambient temperature. The liquid droplets included liquids with various surface tension (Table S1) and kinematic viscosity (dimethyl silicon oil), and a series of non-Newtonian liquids. The non-Newtonian liquids covered milk, tomato sauce, soy sauce, egg white, goat blood, silicone oil, crude oil, sodium alginate (2 wt%) in water, chitosan (2 wt%) in acetic acid solution (1 wt%), PMMA (polymethyl methacrylate, 10 mg mL^{-1}) in DMF (dimethyl formamide), PMMA (10 mg mL^{-1}) in NMP (methyl pyrrolidone), PS (polystyrene, 10 mg mL^{-1}) in DMF, PS (10 mg mL^{-1}) in NMP, PVDF (polyvinylidene fluoride, 10 mg mL^{-1}) in DMF, PVDF (10 mg mL^{-1}) in NMP, PVDF-HFP (poly(vinylidene fluoride-co-hexafluoropropylene, 10 mg mL^{-1}) in DMF, PVDF-HFP (10 mg mL^{-1}) in NMP, PVP (polyvinyl pyrrolidone, 10 mg mL^{-1}) in DMF, PVP (10 mg mL^{-1}) in NMP.

Mechanical durability assessment: Both sandpaper (with 400 mesh)-abrasion and knife-scratch tests by manual operation were used to evaluate the wear resistance of

poc-FPOSS-NP hybrid aggregate-based super-repellent surfaces. With an aim of testing sonication resistance, the super-repellent surfaces were immersed into water and sonicated (power: 480 W) for scheduled times. Using a water blast gun (with outlet pressure of *ca.* 40 bar), the specimens were subjected to continuous impact of water drops at a high speed, which was designed to estimate the liquid-impalement resistance. For assessing the coating adhesion, following the standard ASTM D 3359-09, a commercial tape was applied to the poc-FPOSS-NP hybrid aggregate-based super-repellent surfaces for 60 s (with a loading of 1 kg) and subsequently peeled off (comprising one cycle). At last, the wear resistance, sonication resistance, liquid-impalement resistance and coating adhesion were qualitatively or quantitatively analyzed in terms of contact angle.

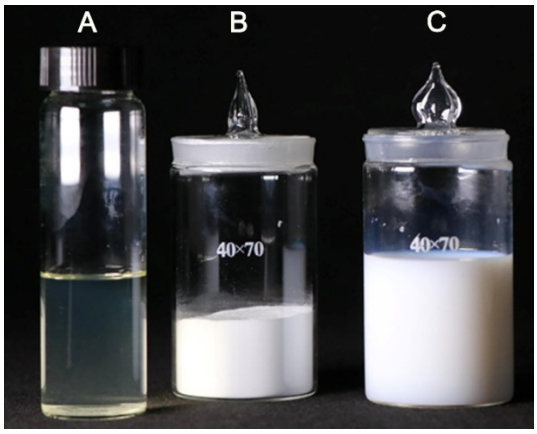

Fig. S1 Photographs of (A) poc-FPOSS-2OH in absolute ethanol, (B) poc-FPOSS-NP hybrid aggregates and (C) suspension containing poc-FPOSS-NP hybrid aggregates and resins.

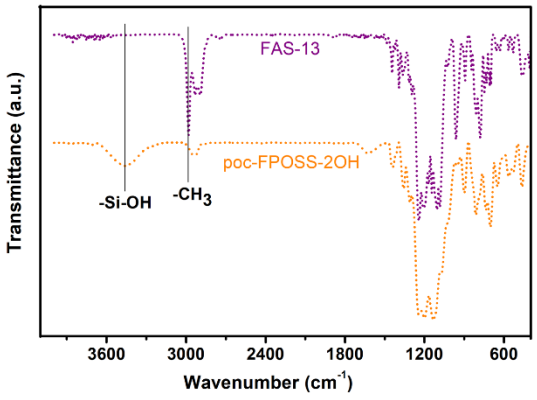

Fig. S2 FTIR spectra of FAS-13 and poc-FPOSS-2OH. In FAS-13 profile, the band at 2975 cm^{-1} was attributed to its stretching vibration of $-CH_3$. In poc-FPOSS-2OH profile, the band at 2975 cm^{-1} disappeared while a new band at 3450 cm^{-1}emerged. The new band could be assigned to stretching vibration of Si-OH. The presence of Si-OH was related with incomplete polycondensation of hydrolyzation (hydrolysate: $(OH)_3C_8H_4F_{13}Si$) of FAS-13 ($(C_2H_5O)_3C_8H_4F_{13}Si$). Obviously, the disappearance of $-CH_3$ band was because of the hydrolyzation of FAS-13 prior to incomplete polycondensation.

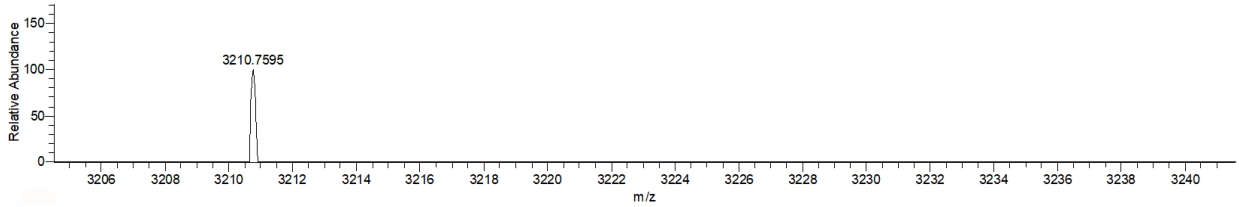

Fig. S3 High resolution mass spectrum of poc-FPOSS-2OH.

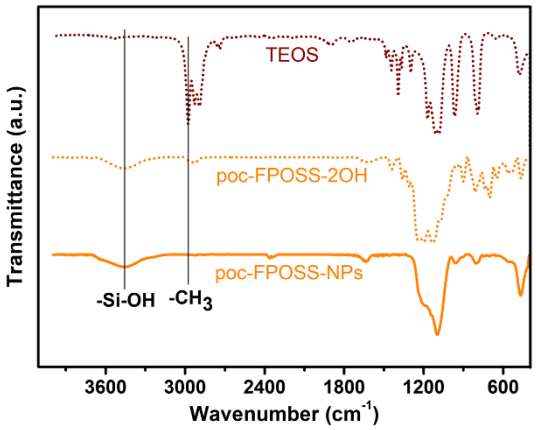

Fig. S4 FTIR spectra of TEOS, poc-FPOSS-2OH and poc-FPOSS-NPs. In TEOS profile, the band at 2975 cm^{-1} was attributed to its stretching vibration of $-CH_3$. In poc-FPOSS-NPs profile, the band at 2975 cm^{-1} disappeared while -OH band of poc-FPOSS-2OH was still there. The disappearance of $-CH_3$ band was because of the hydrolyzation of TEOS prior to copolycondensation. By the combination of Fig. S6, the -OH band of poc-FPOSS-NPs was considered to be directly associated with the superfluous or unreacted -OH of poc-FPOSS-2OH after copolycondensation.

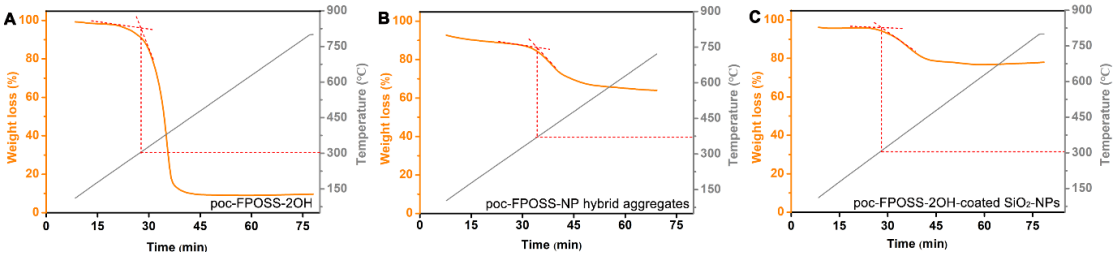

Fig. S5 Thermogravimetric analysis curves of (A) poc-FPOSS-2OH, (B) poc-FPOSS-NP hybrid aggregates and (C) poc-FPOSS-2OH-coated SiO_2-NPs. There is a fact that poc-FPOSS-2OH suffers from poor solubility in acidic ethanol and then is precipitated from acidic ethanol. In absolute ethanol containing poc-FPOSS-2OH and SiO_2-NPs, the dropwise addition of 1M HCl gradually precipitated poc-FPOSS-2OH which was subsequently coated on the surfaces of SiO_2-NPs, and poc-FPOSS-2OH-coated SiO_2-NPs were yielded. According to the three thermogravimetric analysis curves, the poc-FPOSS-2OH, poc-FPOSS-NP hybrid aggregates and poc-FPOSS-2OH-coated SiO_2-NPs started to decompose (fluoroalkyl chains) at *ca.* 305, 370 and 305 °C, respectively. That is to say, regarding the poc-FPOSS-2OH-coated SiO_2-NPs (with same decomposition temperature as poc-FPOSS-2OH), it was a simple physical covering of poc-FPOSS-2OH on SiO_2-NPs, and more importantly, there was no hydrogen bond interaction between poc-FPOSS-2OH and Si-O inorganic chains of SiO_2-NPs. As to the poc-FPOSS-NP hybrid aggregates, the possibility of physical mixing of poc-FPOSS-2OH in nanoparticles had been ruled out by their long-time immersion in absolute ethanol (no loss of poc-FPOSS body was detected). It could be indirectly presumed that poc-FPOSS bodies were covalently bonded in Si-O inorganic chains (by copolycondensation between -OH of poc-FPOSS-2OH and -OH of Si-O oligomers).

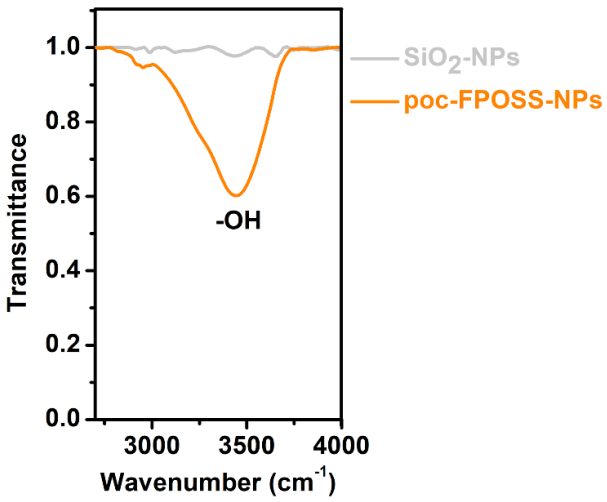

Fig. S6 FTIR spectra (at wavenumber of 2700 ~ 4000 cm^{-1}) of poc-FPOSS-NPs (hybrid aggregates) and SiO_2-NPs. The SiO_2-NPs were obtained under the same preparation conditions as poc-FPOSS-NPs but without using poc-FPOSS-2OH, which, unlike most of common SiO_2-NPs, had hardly any visible band at *ca.* 3450 cm^{-1}. This was probably because the polycondensation of orthosilicic acid $Si(OH)_4$ (hydrolysate of TEOS) was fully completed after dropwise addition of TEOS and 24 h incubation, few -OH survived and appeared on the SiO_2-NP surfaces. Compared with the SiO_2-NPs, the new broad band at *ca.* 3450 cm^{-1} of poc-FPOSS-NPs was assigned to stretching vibration of the superfluous or unreacted -OH of poc-FPOSS-2OH after copolycondensation.

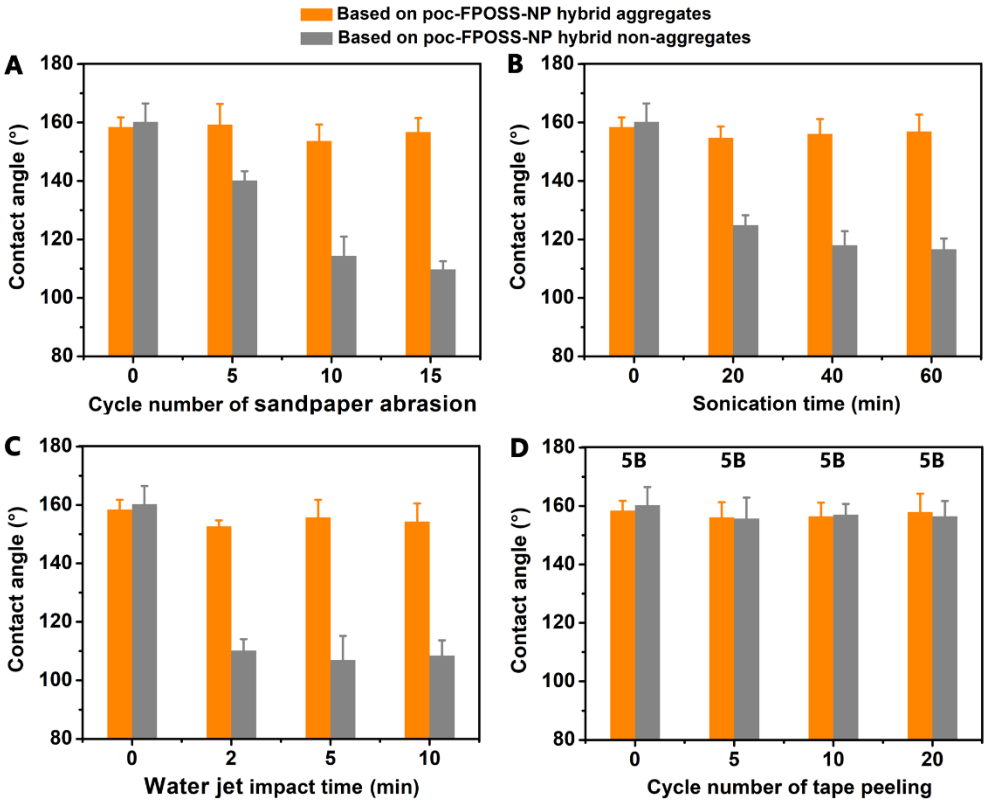

Fig. S7 The plot of contact angle of water on surfaces based on poc-FPOSS-NP hybrid aggregates or poc-FPOSS-NP hybrid non-aggregates *versus* (A) cycle number of sandpaper abrasion, (B) sonication time, (C) water jet impact time and (D) cycle number of tape peeling (5B was the adhesion grade, which was classified by standard ASTM D 3359-09).

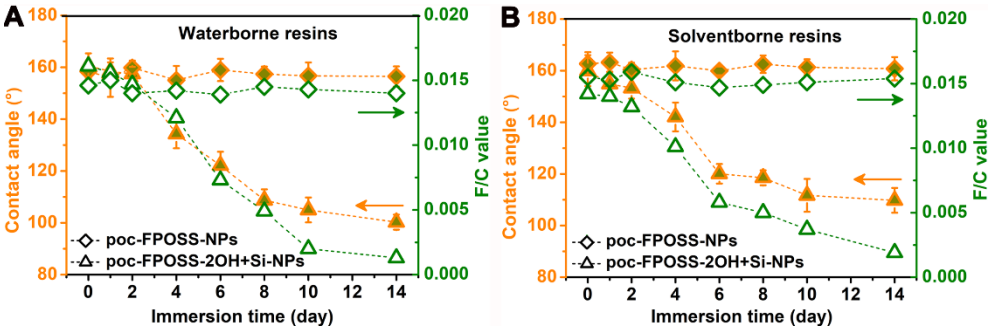

Fig. S8 (A) The plot of contact angle of water and F/C value *versus* immersion time (into flowing water) of surfaces based on waterborne resins and poc-FPOSS-NPs (hybrid aggregates) or Si-NPs. (B) The plot of contact angle of water and F/C value *versus* immersion time (into flowing water) of surfaces based on solventborne resins and poc-FPOSS-NPs (hybrid aggregates) or Si-NPs.

Table S1 List of liquids with various surface tension.

Liquid	**Surface tension** ($mN\ m^{-1}$)	**Liquid**	**Surface tension** ($mN\ m^{-1}$)
Hydrogen peroxide	79.7	Peanut oil	34.5
Water	72.3	n-hexadecane	27.5
Glycerol	63.4	Diesel	26.8
Diiodomethane	50.8	n-dodecane	25.4
Ethylene glycol	48.2	Cyclohexane	24.3
Dimethyl sulfoxide	42.7	n-decane	23.8
N,N-dimethyl formamide	35.6	Polydimethylsiloxane	19.8